Available online at www.sciencedirect.com
ScienceDirect
C. R. Physique 8 (2007) 206–220
COMPTES RENDUS PHYSIQUE
http://france.elsevier.com/direct/COMREN/

Recent advances in crystal optics/Avancées récentes en optique cristalline

Triple photons: a challenge in nonlinear and quantum optics

Kamel Bencheikh [a], Fabien Gravier [b], Julien Douady [c], Ariel Levenson [a], Benoît Boulanger [b,*]

[a] Laboratoire de photonique et de nanostructures, centre national de la recherche scientifique, route de Nozay, 91460 Marcoussis, France
[b] Institut Néel, centre national de la recherche scientifique – université Joseph-Fourier, 25, rue des Martyrs, BP 166, 38042 Grenoble cedex 9, France
[c] Laboratoire de spectrométrie physique, université Joseph-Fourier – centre national de la recherche scientifique, BP 87, 38402 Saint Martin d'Hères, France

Available online 15 September 2006

Invited Paper

Abstract

This article is devoted to the generation and the quantum correlations of triple photons, which correspond to the creation of three highly correlated photons from the splitting of a single photon by a phase-matched third-order parametric nonlinear process. These triples constitute a Greenberger–Horne–Zeilinger state of light and are interesting from a fundamental point of view but also for new schemes of quantum cryptography. We give here the classical and quantum descriptions of triple photon generation, we report on the first experimental demonstration of such a generation, and we calculate the Wigner function of three-photon quantum states of light. ***To cite this article: K. Bencheikh et al., C. R. Physique 8 (2007).***

Résumé

Les triplets de photons : un défi pour l'optique non linéaire et l'optique quantique. Cet article est consacré à la generation et aux corrélations quantiques des triplets de photons. Il s'agit de la création de trois photons fortement corrélés produits à partir de la scission d'un seul photon par un processus non linéaire paramétrique du troisième ordre à l'accord de phase. Ces triplets constituent un état Greenberger–Horne–Zeilinger de la lumière ; ils sont intéressants non seulement d'un point de vue fondamental mais aussi pour de nouveaux protocoles de cryptographie quantique. Nous donnons ici la description à la fois classique et quantique de la génération de triplets de photons, nous décrivons la première démonstration expérimentale d'une telle génération, et nous calculons la fonction de Wigner des états quantiques à 3 photons. ***Pour citer cet article : K. Bencheikh et al., C. R. Physique 8 (2007).***

Keywords: Cubic nonlinear optics; Quantum optics; Nonlinear crystals; Nonclassical states of light; GHZ; Parametric frequency conversion; Quantum correlations; Parametric fluorescence

Mots-clés : Optique non linéaire cubique ; Optique quantique ; Cristaux non linéaires ; États non classiques de la lumière ; GHZ ; Conversion de fréquence paramétrique ; Corrélation quantiques ; Fluorescence paramétrique

* Corresponding author.
E-mail address: benoit.boulanger@grenoble.cnrs.fr (B. Boulanger).

1631-0705/$ – see front matter
doi:10.1016/j.crhy.2006.07.014

1. Introduction: from twin to triple photons

It was only three years after the invention of the laser in 1958 by Arthur L. Schawlow and Charles H. Townes that the first nonlinear optical effect has been observed by Franken et al. [1]. Thanks to the strong electromagnetic field delivered by the 'freshly' invented laser, they observed the birth of a new electromagnetic field oscillating at the second harmonic frequency of the laser field shining on a quartz crystal. This was the beginning of a still ongoing story, where laser and crystal technologies play a major role and in which nonlinear optics reached a high level of maturity. A long road full of fundamental demonstrations and real applications have been achieved. Indeed, nonlinear optical effects such second and third harmonic generation, sum frequency or frequency mixing have become very common.

Quantum mechanically, the development of nonlinear optics allowed the generation and manipulation of new quantum states of light, going from the simplest and common one, the so-called coherent states [2], to squeezed states [3,4], Fock states [5] or entangled states [6].

Among the various nonlinear processes, twin photon generation is one of the most fundamental in manipulating the quantum properties of light. Twin-photon generation is a second order nonlinear process in which a pump photon disappears leading to the creation of two photons with lower energy. This generation is driven by an optical pump field oscillating at the frequency ω_p: it can occur spontaneously, which is called parametric fluorescence, or it can be forced by a seed field oscillating at one or both of the twin photon frequencies; this is the optical parametric amplification, or optical parametric oscillator if the twin photon generation process is enhanced by a resonant cavity.

From the classical point of view, the main interest of a parametric twin beam based process relies in the possibility of obtaining a widely tuneable optical source. Tuneability is associated to the choice of the emission frequency by the phase-matching condition, which corresponds to photon momentum conservation. These types of sources are nowadays commercially available and are widely used in research laboratories. They largely and advantageously expand the spectral regions attained by lasers. Although parametric amplifiers and oscillators are used as 'lasers' in most usual applications, an inherent property makes them deeply different from lasers: in a laser, photons are emitted one-by-one according to Poisson statistics; this is no longer the case in optical parametric twin-photon generators where the photons are emitted by pairs, altering drastically their behaviour at the very heart of several non classical properties, such as second order coherence, quantum correlations between the twins, squeezing of quantum fluctuations and, the more intriguing, quantum entanglement. Besides the tuneable optical parametric sources that are widely developed nowadays, these quantum aspects constitute the key feature in huge number of demonstrations such as noiseless optical amplification [7], quantum cryptography [8] and quantum teleportation [9].

Since the twin photons have deeply influenced the history of nonlinear and quantum optics by their wide range of applications and their paradigmatic place they stand in generating new quantum states of light, we can ask whether the properties of triple photons can play a similar major role in the future of nonlinear and quantum optics.

From the classical point of view, triple photon generation is a real challenge. Indeed, a few attempts have been made in the past ten years, but without any success. These failures were due in part to the weak magnitude of the third order electric susceptibility, but also to partial knowledge of the specific of the corresponding processes, which cannot be deduced from a simple analogy with second order interactions. The most symptomatic feature deals with the phase-matching properties, since a third order parametric fluorescence would generate a broad continuum instead of discrete wavelengths, which leads to a huge spreading of the energy and thus to a weak amount of photons *per* generated spectral component. This behaviour is due to the existence of only two equations, i.e. the energy and momentum conservations, to fix the values of three parameters, i.e. the wavelengths of the three generated photons. The development of the classical theory of the third order nonlinear parametric interactions is then the starting point, from which it will be possible to define the most suitable schemes to achieve an efficient triple photon generation and hence to perform quantum experiments.

Quantum mechanically, triple photon generation is obviously the most direct way to produce pure quantum states of light whose statistics go beyond the usual Gaussian statistics associated with coherent sources and optical parametric twin-photon generators. The simultaneous birth of three photons is indeed at the origin of intrinsic three-body quantum properties such as three-particle Greenberger–Horne–Zeilinger quantum entanglement and Wigner functions presenting quantum interferences and negativities.

From the seminal work of [10,11] on optical parametric conversion to the nowadays mature sources for both classical and quantum optical applications, a long road has been covered thanks to the development of a classical and a quantum theoretical framework that has allowed one to drive the experimental efforts, and thanks to the development of high-quality and highly second order nonlinear optical materials. As regards three-photon generation, the story is only starting and efficient third order nonlinear materials beyond three-photon generation as efficient as those permitting twin-photon generation are not yet available.

In this article, we consider the generation of triple photons where a pump field incident on a nonlinear material gives birth simultaneously to three photons. We give a classical description of the phenomenon and a realistic scheme that lead to the first experimental demonstration of an optical parametric amplification based on three-photon generation in a KTP crystal. Furthermore, we calculate the efficiency of a third order parametric fluorescence process, and we address, through the calculation of the Wigner function, the quantum properties of three-photon quantum states of light, showing their purely non classical behaviour.

2. Classical theory of parametric third-order nonlinear optics

Two possible schemes of third-order nonlinear optical interactions can be distinguished according to energy conservation:

$$\hbar\omega_0 + \hbar\omega_1 = \hbar\omega_2 + \hbar\omega_3 \tag{1}$$

$$\hbar\omega_0 = \hbar\omega_1 + \hbar\omega_2 + \hbar\omega_3 \tag{2}$$

Relation (1) corresponds to a wide range of nonlinear processes such as a nonlinear index, two-photon absorption, solitons, phase conjugation, four-wave mixing or Raman scattering, for example. These interactions are not able to produce photon triples, since none of the four photons involved have an energy equal to the sum of the energy of the three others, contrary to the situations described by relation (2). Actually in this last case, the splitting of a photon at $\hbar\omega_0$ can lead to the generation of three lower-energy photons at $\hbar\omega_1$, $\hbar\omega_2$ and $\hbar\omega_3$, which corresponds to third order parametric fluorescence as shown in Fig. 1.

Note that third order sum-frequency generation, like third harmonic generation for example, is the reverse process of triple photon generation: it is also described by relation (2), but it corresponds to the fusion of three incoming photons at $\hbar\omega_1$, $\hbar\omega_2$ and $\hbar\omega_3$, leading to the generation of a photon at $\hbar\omega_0$.

The Cartesian coordinates of the four spectral components of the macroscopic third order electronic polarization of a unit volume corresponding to a nonlinear process described by relation (2) are given by [12]:

$$P_i^{(3)}(\omega_a) = \varepsilon_0 \cdot \sum_{j,k,l} \big(\chi_{ijkl}^{(3)}(\omega_a = \omega_b + \omega_c + \omega_d) \cdot E_j(\omega_b) \cdot E_k(\omega_c) \cdot E_l(\omega_d)\big) \tag{3}$$

with $\{\omega_b, \omega_c, \omega_d\} = \{\omega_1, \omega_2, \omega_3\}, \{\omega_0, -\omega_2, -\omega_3\}, \{\omega_0, -\omega_1, -\omega_3\}, \{\omega_0, -\omega_1, -\omega_2\}$ for $\omega_a = \omega_0, \omega_1, \omega_2, \omega_3$ respectively; the Cartesian indices i, j, k, and l are relative to the optical frame (O, x, y, z), the E_α are the components of the complex amplitudes of the electric fields of the four interacting waves, and the $\chi_{ijkl}^{(3)}$ are the components of the third order electric susceptibility tensor of the medium at the different circular frequencies.

$\chi^{(3)}$ is a rank-four polar tensor: it has 81 independent components in the general case, but Kleinmann approximation and the orientation symmetry of the medium according to the Neumann principle allow us to reduce this

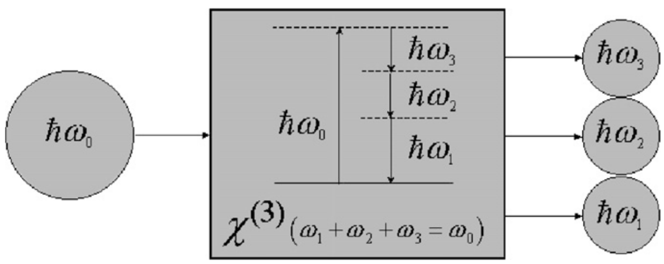

Fig. 1. Photonic diagram of the parametric fluorescence governed by the third order electric susceptibility $\chi^{(3)}$: an incoming photon at $\hbar\omega_0$ is splitted into three photons at $\hbar\omega_1$, $\hbar\omega_2$ and $\hbar\omega_3$ in the nonlinear medium.

number [13]. Both centrosymmetric and noncentrosymmetric crystal classes have a nonzero third order electric susceptibility, its magnitude being very weak and ranging typically between 10^{-21} m^2/V^2 and 10^{-19} m^2/V^2 [14].

In the case of non magnetic and non-conducting medium, the resolution of Maxwell equations leads to the following propagation equations for each of the four interacting waves:

$$\overrightarrow{\mathrm{rot}}\big(\overrightarrow{\mathrm{rot}}\big(\vec{E}(\omega_i)\big)\big) + \mu_0 \cdot \varepsilon_0 \cdot \varepsilon_r(\omega_i) \cdot \frac{\partial^2 \vec{E}(\omega_i)}{\partial t^2} = \mu_0 \cdot \frac{\partial^2 \vec{P}^{(3)}}{\partial t^2} \tag{4}$$

where $i = 0, 1, 2$, or 3, and the Cartesian components of $\vec{P}^{(3)}$ are given by (3).

By considering that the four interacting waves propagate in the same direction, Z, by neglecting the absorption and by assuming the slowly varying envelope and ABDP approximation, i.e., $\chi^{(3)}_{ijkl}(\omega_0 = \omega_1 + \omega_2 + \omega_3) = \chi^{(3)}_{jikl}(\omega_1 = \omega_0 - \omega_2 - \omega_3) = \chi^{(3)}_{kijl}(\omega_2 = \omega_0 - \omega_1 - \omega_3) = \chi^{(3)}_{lijk}(\omega_3 = \omega_0 - \omega_1 - \omega_2)$ Eq. (4) leads to the following coupled system:

$$\frac{\partial E(\omega_a)}{\partial Z} = j \cdot \frac{\pi \cdot \chi^{(3)}_{\mathrm{eff}}}{n(\omega_a) \cdot \lambda_a . \cos(\gamma(\omega_a))} \cdot E(\omega_b) \cdot E(\omega_c) \cdot E(\omega_d) \cdot \mathrm{e}^{j.\xi.\Delta k.Z} \tag{5}$$

with $\{\omega_b, \omega_c, \omega_d, \xi\} = \{\omega_1, \omega_2, \omega_3, -1\}$, $\{\omega_0, -\omega_2, -\omega_3 + 1\}$, $\{\omega_0, -\omega_1, -\omega_3, +1\}$, $\{\omega_0, -\omega_1, -\omega_2, +1\}$ for $\omega_a = \omega_0, \omega_1, \omega_2, \omega_3$ respectively.

$n(\omega_i)$ is the refractive index corresponding to $E(\omega_i)$, $\lambda_i = \frac{2\pi \cdot c}{\omega_i}$ is the wavelength associated with ω_i, and $\gamma(\omega_i)$ is the walk-off angle corresponding to the double refraction effect.

The effective coefficient, $\chi^{(3)}_{\mathrm{eff}}$, is the contraction between the third order electric susceptibility tensor $\chi^{(3)}$ and the field tensor $F^{(3)}$ [13]:

$$\chi^{(3)}_{\mathrm{eff}} = \chi^{(3)} \cdot F^{(3)} \tag{6}$$

where $F^{(3)}$ is also a rank-four tensor expressed as the tensorial product $\otimes$ between the unit electric field vectors of the four interacting waves:

$$F^{(3)} = \vec{e}(\omega_0) \otimes \vec{e}(\omega_1) \otimes \vec{e}(\omega_2) \otimes \vec{e}(\omega_3) \tag{7}$$

The symmetry and the components of the field tensor are directly linked with the configuration of polarization of the nonlinear process, and thus they are trigonometric functions of the direction of propagation [13]. So the effective coefficient depends on both the linear and nonlinear optical properties.

The phase mismatch Δk is given by:

$$\Delta k = k_0 - k_1 - k_2 - k_3 \tag{8}$$

where $k_i = \frac{\omega_i}{c} n(\omega_i)$ is the modulus of the wave vector associated with $\vec{E}(\omega_i)$. The product $\Delta k \cdot Z$ represents the dephasing between the nonlinear polarization $\vec{P}^{(3)}(\omega_i)$ and the corresponding radiated electric field $\vec{E}(\omega_i)$. The transfer of energy between the interacting waves is maximum for $\Delta k = 0$, which defines phase-matching: it is realized by the matching of the refractive indices using birefringence of anisotropic media. Phase-matching can be achieved only if the direction of propagation has a birefringence that compensates the dispersion. Except for a propagation along the optical axis, there are two possible values, n^+ and n^-, which are the two solutions of the Fresnel equation [13], for each of the four refractive indices involved in relation (8). Thus, there are 2^4 possible combinations of refractive indices, but only 7 are compatible with both the dispersion in frequency, the phase-matching relation (8) and the energy conservation (2): $\{-,+,+,+\}$, $\{-,-,-,+\}$, $\{-,-,+,-\}$, $\{-,+,-,-\}$, $\{-,-,+,+\}$, $\{-,+,-,+\}$ and $\{-,+,+,-\}$ corresponding to $\{n(\omega_0), n(\omega_1), n(\omega_2), n(\omega_3)\}$ [13]. The loci of the phase-matching direction of each of these configurations are calculated by using the corresponding phase-matching relation and the dispersion equations of the principal refractive indices of the considered crystal. Note that from the point of view of the quantum theory of light, the phase-matching of the waves corresponds to the total photon-momentum conservation, i.e. $\hbar\vec{k}_0 = \hbar\vec{k}_1 + \hbar\vec{k}_2 + \hbar\vec{k}_3$. For a fixed direction of propagation and a given pump wavelength λ_0, the triple $(\lambda_1, \lambda_2, \lambda_3)$ generated by parametric fluorescence is not a single one but is spread over a broad continuum. Actually, there are only two coupled relations, i.e. the energy and the momentum conservations, for the determination of three unknown values. Note that it is different in the case of the second order parametric fluorescence for which there are only two unknown values. Fig. 2 gives the example of a propagation along x-axis in a $KTiOPO_4$ crystal with $\lambda_0 = 532$ nm and with the following configuration: $\lambda_0^{(-)} \to \lambda_1^{(+)} + \lambda_2^{(-)} + \lambda_3^{(+)}$.

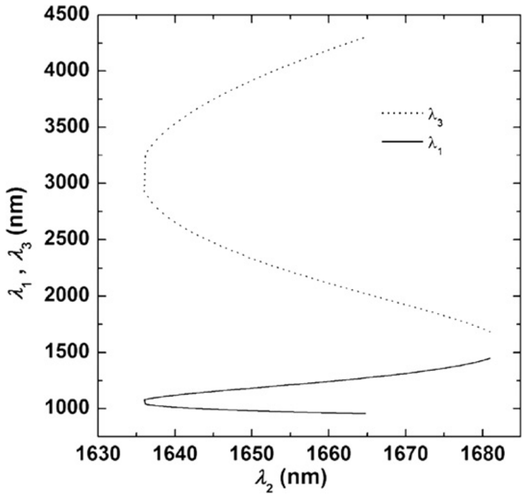

Fig. 2. Calculated phase-matching curves corresponding to the parametric fluorescence $\lambda_0^{(-)} \to \lambda_1^{(+)} + \lambda_2^{(-)} + \lambda_3^{(+)}$ along x-axis of KTP pumped at $\lambda_0 = 532$ nm.

The calculations show a huge spreading, which covers the range 950 to 4500 nm. Such a situation is strongly detrimental to our objective. Actually, it is necessary to concentrate the energy on a single triple if we want to be able to make any observation and measurement, all the more so since the amplitude of $\chi^{(3)}$ is weak. An alternative to avoid any spreading is to fix the value of the wavelength of one photon of the triple: it can be done by irradiating the nonlinear medium with the pump beam at λ_0 and an injection beam at λ_1, λ_2 or λ_3. This process corresponds to a parametric difference-frequency mixing. From the quantum point of view, this process can be seen as the stimulated splitting of the pump photon by the injection photon, and thus the corresponding generated optical state contains a mix of $(\omega_1, \omega_2, \omega_3)$ triple photons and injection photons at ω_1, ω_2 or ω_3. Note that the triple generation can also be stimulated by two injection photons.

Contrary to $\chi^{(2)}$ processes, the quasi-phase-matching of $\chi^{(3)}$ interactions is not possible in periodically poled crystals such as PPLN and PPKTP, or any other ferroelectric crystals: the technique of Z-axis reversal does not lead to the reversal of the sign of the highest third order nonlinear coefficient, $\chi^{(3)}_{zzzz}$, since this coefficient is relative to an even number of the Z-Cartesian index. Note that in the case of an odd number, the quasi-phase-matching of a third order parametric process would be possible.

The complex electric field amplitudes in Eq. (5) are written $E(\omega_i) = |E(\omega_i)| \cdot e^{j\phi_i}$, where i stands for 0, 1, 2 and 3, and the angles ϕ_i correspond to the initial phases. In the case of phase-matching, i.e. $\Delta k = 0$, system (5) becomes:

$$\frac{\partial |E(\omega_a)| \cdot e^{j\phi a}}{\partial Z} = j \cdot \frac{\pi \cdot \chi^{(3)}_{\mathrm{eff}}}{n(\omega_a) \cdot \lambda_a \cdot \cos(\gamma(\omega_a))} \cdot \left|E(\omega_b)\right| \cdot \left|E(\omega_c)\right| \cdot \left|E(\omega_d)\right| \cdot e^{j(\phi_b+\phi_c+\phi_d)} \tag{9}$$

with $\{(\omega_b, \phi_b), (\omega_c, \phi_c), (\omega_d, \phi_d)\} = \{(\omega_1, \phi_1), (\omega_2, \phi_2), (\omega_3, \phi_3)\}$, $\{(\omega_0, \phi_0), (-\omega_2, -\phi_2), (-\omega_3, -\phi_3)\}$, $\{(\omega_0, \phi_0), (-\omega_1, -\phi_1), (-\omega_3, -\phi_3)\}$, $\{(\omega_0, \phi_0), (-\omega_1, -\phi_1), (-\omega_2, -\phi_2)\}$ for $\omega_a = \omega_0, \omega_1, \omega_2, \omega_3$, respectively.

In the case of the generation of triple photons, which corresponds to $\frac{\partial |E(\omega_0)|}{\partial Z} < 0$ and $\frac{\partial |E(\omega_{i\neq 0})|}{\partial Z} > 0$, the initial phases are necessary locked such as $\phi_0 - \phi_1 - \phi_2 - \phi_3 = -\pi/2$. This situation is considered for the following calculations.

We take the example of a triple photon generation pumped at ω_0 and stimulated by two injection photons at ω_1 and ω_2, which corresponds to $|E(\omega_{i\neq 1}, Z = 0)| \neq 0$ and to $|E(\omega_1, Z = 0)| = 0$. Then the integration of Eqs. (9) over the crystal length L leads to the intensity of each of the four interacting beams, according to $I(\omega_i, Z = L) = \frac{1}{2} n(\omega_i) \sqrt{\frac{\varepsilon_0}{\mu_0}} |E(\omega_i, Z = L)|^2$ [15]:

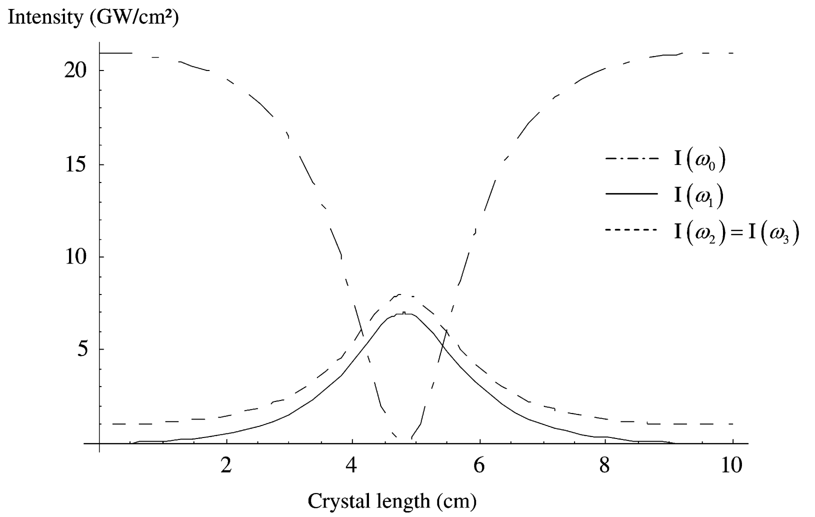

Fig. 3. Calculated intensities of a phase-matched parametric third order frequency mixing along the direction of propagation in a KTP crystal; $\omega_0 = 3\omega$, $\omega_1 = \omega_2 = \omega_3 = \omega$.

$$\begin{cases} I(\omega_0, Z = L) = \dfrac{I(\omega_0, Z = 0) \cdot (\gamma_{31} + \gamma_{01}) \cdot cn^2(a_1 \cdot L|1 - m_1)}{\Gamma} \\ I(\omega_1, Z = L) = \dfrac{\gamma_{31} \cdot \gamma_{01} \cdot sn^2(a_1 \cdot L|1 - m_1)}{\Gamma} \\ I(\omega_{2,3}, Z = L) = \dfrac{I(\omega_{2,3}, Z = 0) \cdot (\gamma_{31} + \gamma_{01}) \cdot (\beta_{2,3} \cdot sn^2(a_1 \cdot L|1 - m_1) + cn^2(a_1 \cdot L|1 - m_1))}{\Gamma} \end{cases} \tag{10}$$

where $sn(u|m)$ and $cn(u|m)$ are Jacobi elliptic functions,

$$\Gamma = \gamma_{31} \cdot m_1 \cdot sn^2(a_1 \cdot L|1 - m_1) + (\gamma_{31} + \gamma_{01}) \cdot cn^2(a_1 \cdot L|1 - m_1)$$

$$\gamma_{ij} = \frac{\lambda_i}{\lambda_j} I(\omega_i, Z = 0) + I(\omega_j, Z = 0)$$

$$\beta_2 = 1, \ \beta_3 = m_1 \text{ with } m_1 = \frac{\gamma_{21} \cdot (\gamma_{01} + \gamma_{31})}{\gamma_{31} \cdot (\gamma_{01} + \gamma_{21})}, \text{ and}$$

$$a_1 = \frac{\Lambda_1}{2} \cdot \sqrt{\gamma_{31} \cdot (\gamma_{01} + \gamma_{21})} \text{ with } \Lambda_1 = \sqrt{\frac{\mu_0}{\varepsilon_0}} \cdot \frac{4\pi \cdot \chi_{\text{eff}}^{(3)}}{\sqrt{n(\omega_0) \cdot n(\omega_1) \cdot n(\omega_2) \cdot n(\omega_3)}} \cdot \sqrt{\frac{\lambda_1}{\lambda_0 \cdot \lambda_2 \cdot \lambda_3}}$$

We consider as a numerical example the interaction $3\omega^- \to \omega^+ + \omega^+ + \omega^-$, with $\lambda_\omega = 1620$ nm, $I(\omega_0 = 3\omega, Z = 0) = 21\ \text{GW/cm}^2$ and $I(\omega_2 = \omega, Z = 0) = I(\omega_3 = \omega, Z = 0) = 1\ \text{GW/cm}^2$, phase-matched along the X-axis of KTP. The corresponding curves are plotted in Fig. 3.

According to the periodic evolution of the Jacobi elliptic functions, the intensities of the four interacting fields have a periodic evolution: the photon fusion $\omega^+ + \omega^+ + \omega^- \to 3\omega^-$ starts up when the pump at 3ω is completely depleted by the splitting $3\omega^- \to \omega^+ + \omega^+ + \omega^-$, and so on. That kind of behaviour is the same than for the second order parametric interactions [16].

Having established the main theoretical framework able to describe classically the three-photon generation, we will in the next section address the quantum aspect of three-photon generation.

3. Parametric three-photon fluorescence

The generated three photons are analogous to the Greenberger–Horne–Zeilinger (GHZ) states. They are very attractive because of their three-body quantum correlations that can find a wide range of applications in quantum information domain and more particularly in quantum cryptography. The starting point to the quantum description of three-photon generation is the estimation of the number of the triplets generated in the fluorescence process by which a pump photon with energy $\hbar\omega_0$ incident on a third order nonlinear crystal splits into three highly correlated photons following the energy conservation relation given by Eq. (2), and the photon momentum conservation:

$$\vec{k}_0 = \vec{k}_1 + \vec{k}_2 + \vec{k}_3 \tag{11}$$

In this process, the only fixed quantities are the pump frequency ω_0 and the pump momentum vector $\vec{k}_0$. The determination of the fluorescence power is based on the Fermi golden rule [17]

$$W = \frac{2\pi}{\hbar}\left|\langle\vec{k}_1, \vec{k}_2, \vec{k}_3\big|\widehat{H}_i|0,0,0\rangle\right|^2 \rho \tag{12}$$

that gives the rate of transition from the three-photon quantum state $|0,0,0\rangle$ containing no photons in each mode to the three-photon quantum state $|\vec{k}_1, \vec{k}_2, \vec{k}_3\rangle$ with a single photon having a momentum $\vec{k}_i$ in each of the three modes. In Eq. (12), ρ is the density per unit energy of the final states and the Hamiltonian $\widehat{H}_i$ describes the third order nonlinear interaction process responsible of the generation of triple photons. It is expressed as following:

$$\widehat{H}_i = \frac{3}{4}\varepsilon_0\chi^{(3)}\left(\frac{2\hbar}{\varepsilon_0 L^3}\right)^2 \frac{\sqrt{\omega_0\omega_1\omega_2\omega_3}}{n_0 n_1 n_2 n_3}\alpha_0 \int \mathrm{d}^3\vec{r}\,\left(f(\vec{r})\hat{a}_1^+\hat{a}_2^+\hat{a}_3^+\mathrm{e}^{+i\Delta\vec{k}.\vec{r}-\mathrm{i}\Delta\omega t} + \text{h.c.}\right) \tag{13}$$

where h.c. denotes the Hermitian conjugate. α_0 is a complex number representing the amplitude of the pump field that is supposed strong enough to be described classically; $\hat{a}_i^+$ $(i = 1,2,3)$ are the creation operators describing the triple photons, L^3 is the quantification volume and $f(\vec{r}) = \sqrt{2/\pi}(L/w_0)\exp(-\vec{r}^2/w_0^2)$ is a normalization function that accounts for the Gaussian profile of the pump field having a waist size w_0. In Eq. (13), the quantities $\Delta\vec{k} = \vec{k}_0 - \vec{k}_1 - \vec{k}_2 - \vec{k}_3$ and $\Delta\omega = \omega_0 - \omega_1 - \omega_2 - \omega_3$ denote the photon-momentum and the energy mismatches, respectively.

The density of final states per unit energy is deduced from the number of modes contained in the element $\mathrm{d}^3\vec{k}_1\,\mathrm{d}^3\vec{k}_2\,\mathrm{d}^3\vec{k}_3$. It is given by:

$$\rho = \frac{1}{(2\pi/L^3)^3}\left(\frac{n_1}{\hbar c}\right)^3 E_1^2\,\mathrm{d}^3\vec{k}_2\,\mathrm{d}^3\vec{k}_3 \tag{14}$$

where $E_1 = \hbar\omega_1$ and $2\pi/L^3$ being the elementary volume occupied by a single mode. The radiated power in the frequency interval $\mathrm{d}\omega_2$ along the direction $\vec{k}_2$ within the solid angle $\mathrm{d}\Omega_2$ is obtained by multiplying (12) by $\hbar\omega_2$ and integrating over $\mathrm{d}^3\vec{k}_3$. Using (12)–(14), we obtain:

$$\begin{aligned} P_2 &= \frac{9\hbar^2}{128\pi^4\varepsilon_0^2 c^7}\left[\chi^{(3)}\right]^2\frac{n_1 n_2}{n_0 n_3^2}P_0 L_{\text{int}}\omega_1^3\omega_2^4\omega_3\,\mathrm{d}\omega_2\,\mathrm{d}\Omega_2 \\ &= \frac{288\hbar^2\pi^5 c^2}{8\varepsilon_0^2}\left[\chi^{(3)}\right]^2\frac{n_1 n_2}{n_0 n_3^2}P_0 L_{\text{int}}\frac{\mathrm{d}\lambda_2\,\mathrm{d}\Omega_2}{\lambda_1^3\lambda_2^6\lambda_3} \end{aligned} \tag{15}$$

For comparison, we recall the expression of the integrated signal power generated in the case of twin-photon parametric fluorescence $\omega_P \to \omega_s + \omega_i$ [17]:

$$P_s = \frac{\hbar}{\pi\varepsilon_0 c^3}\frac{d^2}{n_p^2}P_p L_{\text{int}}\frac{\omega_s^3\omega_i^2}{\omega_p}\,\mathrm{d}\omega_s = \frac{32\hbar\pi^4 c}{\varepsilon_0}\frac{d^2}{n_p^2}P_p L_{\text{int}}\frac{\lambda_p}{\lambda_s^5\lambda_i^2}\,\mathrm{d}\lambda_s \tag{16}$$

where the subscripts p, s and i stand for the pump, signal and idler photons, respectively; d is the effective second order nonlinear coefficient. Eq. (16) can be compared to Eq. (15), making abstraction of the solid angle $\mathrm{d}\Omega_2$, which vanishes after the integration.

As in the case of twin-photon, triple-photon parametric fluorescence is proportional to the pump power and to the interaction length L_{int}. However, Eq. (15) shows that the generated power varies like the reciprocal of the tenth power of the triple-photons wavelengths. In comparison, the fluorescence power of the generated twin-photons given by (16) shows a dependence to the inverse of the seventh power of the twin-photons wavelengths. Though the efficiency is strongly dependent on the wavelength, triple-photon generation is more severely limited by the rather low values of the third order nonlinear susceptibility, i.e. $\chi^{(3)} \approx 10^{-21}\ \mathrm{m}^2/\mathrm{V}^2$, of the most known materials at present days.

Considering the laser source and nonlinear crystal that are used in the present study, we can easily make an estimate from Eq. (15) of the number of triplets we expect to generate with the maximum available pump intensity of about

350 GW/cm^2, corresponding to a pump power $P_0 = 37$ MW, within the 25-mm-long KTP crystal. For simplicity, we suppose that all three wavelengths are equal and are taken to be $\lambda_1 = \lambda_2 = \lambda_3 \approx 1665$ nm. For a detection bandwith $\mathrm{d}\lambda = 50$ nm and $\mathrm{d}\Omega = 10^{-5}$ str, we find that the generated power is about $P_2 \approx 3 \times 10^{-17}$ W, which is very low to be detected. Indeed, if we consider a 10 Hz repetition rate and a 22 ps pulse duration laser source, we expect to produce less than 0.01 triplets *per* day, whereas, according to Eq. (16), about 10^6 twins *per* day are generated if we consider the twin-photon generation process in the same KTP crystal pumped with same pump power at 532 nm and when the phase-matching condition is fulfilled in order to produce degenerate twin photons at 1064 nm, the second order nonlinear susceptibility of the crystal being taken at $d \approx 1$ pm/V. At this stage, the efficiency of triple-photon parametric fluorescence is still very low in comparison with twin-photon fluorescence. This prevents us performing any parametric fluorescence experiments to detect the triplets and studying their quantum properties.

Thus the main conclusion of this quantum description is that it will be necessary to stimulate the photon splitting to achieve an efficient triple photon generation, as proposed above within the framework of the classical description on the basis of the phase-matching analysis.

4. Three-photon quantum states of light

A full quantum theoretical analysis of the three-photon states is contained in the Wigner function [18]:

$$W(q,p) = \frac{1}{2\pi} \int_{-\infty}^{+\infty} \mathrm{e}^{\mathrm{i}px} \langle q - x/2|\hat{\rho}|q + x/2\rangle \,\mathrm{d}x \tag{17}$$

that has proven to be very helpful to visualize in the phase space — the amplitude q and phase p quadratures — quantum mechanical system defined by its density matrix $\hat{\rho} = |\psi\rangle\langle\psi|$. This has already been the case for some quantum states of light such as the coherent state, the squeezed vacuum or the bright squeezed state [19,20], whose Wigner function has been experimental reconstructed using homodyne quantum tomography, a technique that allows the measurement of the marginal probability distribution

$$P(q,\theta) = \frac{1}{2\pi} \int_{-\infty}^{+\infty} W(q\cos\theta - p\sin\theta, q\sin\theta + p\cos\theta) \,\mathrm{d}p \tag{18}$$

that expresses the quadrature amplitude distribution.

More generally, the Wigner function contains the full information about the quantum states. More particularly, it allows us to establish the quantum correlations between the different generated modes in the case of twin photons or photon triplets. The Wigner function is a positive definite function in the phase space for classical states with Gaussian marginal probability distributions. However, it can be negative in some circumstances for particular quantum states of light. These negativities are the signature of highly nonclassical behaviour of a quantum state as it has been observed for a quantum state of light prepared in a single-photon Fock state [5]. These quantum negativities are also present in the case of complete degenerate three-photon states obtained by third order optical parametric fluorescence or amplification. This particular case has been investigated by K. Banaszek et al. [21] and T. Felbinger et al. [22], who showed that the Wigner function has a shape of star with three branches in the phase space.

According to the definition (17), the knowledge of the Wigner function depends on the determination of the density operator of the quantum state and thus on the determination of the wave function itself:

$$\left|\psi(t)\right\rangle = \mathrm{e}^{\mathrm{i}\widehat{H}_i t/\hbar}\left|\psi(0)\right\rangle \tag{19}$$

where $\widehat{H}_i = \hbar g(\hat{a}_p\hat{a}_e^{+2}\hat{a}_o^{+} + \hat{a}_p^{+}\hat{a}_o^{2}\hat{a}_e)$ is the interaction Hamiltonian accounting for the nonlinear process through the third order nonlinear coefficient g proportional to $\chi^{(3)}$ and where the annihilation (creation) of a pump photon leads to the creation (annihilation) of two photons in the extraordinary mode e and one photon in the ordinary mode o. Here, we consider the relevant situation where 2 photons (called e) out of 3 are degenerate. We also suppose that all three photons have the same energy $\hbar\omega$. This particular configuration is suited to describe theoretically the experimental situation of the next section. The two degenerate e modes are easily obtained by a linear superposition of the modes $\lambda_2^+ = \lambda_3^- = 1665$nm. The o mode is that corresponding to $\lambda_1^- = 1474$ nm.

At instant $t = 0$, the wave function of the quantum system can be decomposed as:

$$\big|\psi(0)\big\rangle = |\beta, \alpha, 0\rangle = \sum_{n=0}^{\infty}\sum_{m=0}^{\infty} \mathrm{e}^{-(|\beta|^2+|\alpha|^2)/2} \frac{\beta^n \alpha^m}{\sqrt{n!m!}} |n, m, 0\rangle \tag{20}$$

where the pump and extraordinary modes are considered to be coherent states $|\beta\rangle$ and $|\alpha\rangle$. The state $|n, m, 0\rangle = |n\rangle|m\rangle|0\rangle$ is the product of the Fock states with n photon in the pump mode, m photon in the extraordinary mode and no photon in the ordinary mode. The case $|\alpha \neq 0\rangle$ corresponds to the injection at $\lambda_2^+ = \lambda_3^- = 1665$ nm in the seeded KTP-based optical parametric amplifier. The particular situation of no photon in the extraordinary mode can easy be deduced by reducing the sum over m to the first term $m = 0$. Since the free-field Hamiltonian $\widehat{H}_0 = 3\hbar\omega\hat{a}_p^+\hat{a}_p + 2\hbar\omega\hat{a}_e^+\hat{a}_e + \hbar\omega\hat{a}_o^+\hat{a}_o$ is a constant of motion, the total photon number $3\langle\hat{a}_p^+\hat{a}_p\rangle + 2\langle\hat{a}_e^+\hat{a}_e\rangle + \langle\hat{a}_o^+\hat{a}_o\rangle$ is conserved. Moreover, it is easy to show that the set of quantum states $\vec{\Psi}^T = \{|n-k, m+2k, k\rangle,\ k = 0, \ldots, n\}$ are eigenstates of the Hamiltonian $\widehat{H}_0$. Our calculations of the Wigner function corresponding to the state (19) are inspired by the pioneering work of D.F. Walls and R. Barakat in the early 1970s [23]. A preliminary step is the calculation of the state $|\psi(t)\rangle$ itself. This is done by first computing the eigenstates and the eigenvalues of the interaction Hamiltonian $\widehat{H}_i$, or in other words diagonalize the $(n+1)\times(n+1)$ matrix A such that:

$$H_i\vec{\Psi}^T = \hbar g A.\vec{\Psi}^T \tag{21}$$

and where:

$$A = \begin{pmatrix} 0 & a_1 & & & \cdots & & 0 \\ a_1 & 0 & a_2 & & & & \\ 0 & a_2 & 0 & a_3 & & & \vdots \\ & & & \ddots & & & \\ \vdots & & & & \ddots & & 0 \\ 0 & & \cdots & 0 & a_{n-1} & 0 & a_n \\ 0 & & \cdots & & 0 & a_n & 0 \end{pmatrix} \tag{22}$$

with $a_l = \sqrt{(n-k+l)(m+2l+1)(m+2l+2)l}$, $l = 1, \ldots, n$.

The eigenstates $\vec{\Phi}$ of the Hamiltonian $\widehat{H}_i$ are linear superpositions of the free-field Hamiltonian eigenstates $\vec{\Psi}$. This is expressed through the relation $\vec{\Phi}^T = U.\vec{\Psi}^T$ where U is a $(n+1)\times(n+1)$ matrix whose each row i elements are the eigenstates of the matrix A with the eigenvalue λ_i. After some mathematical manipulations, we deduce the three-photon quantum state:

$$\big|\psi(t)\big\rangle = \mathrm{e}^{-(|\beta|^2+|\alpha|^2)/2} \sum_{n=0}^{\infty}\sum_{m=0}^{\infty}\sum_{l=1}^{n+1}\sum_{k=0}^{n} \frac{\beta^n\alpha^m}{\sqrt{n!m!}} \mathrm{e}^{-\mathrm{i}r\lambda_l} u_{l,1}u_{l,k+1}|n-k, m+2k, k\rangle \tag{23}$$

where $r = g \times t$, with t being the interaction time, and $u_{i,j}$ are the matrix U elements. Eq. (23) expresses that the final quantum state can be written as a complex linear superposition of the Fock states $|n-k, m+2k, k\rangle$.

Fig. 4 shows the so-called star state Wigner function in the case of completely degenerate three photons generation. This Wigner function is obtained by setting $\alpha = 1$ and $m = 0$ in Eq. (23). We obtain:

$$\big|\psi(t)\big\rangle = \mathrm{e}^{-|\beta|^2/2} \sum_{n=0}^{\infty}\sum_{l=1}^{n+1}\sum_{k=0}^{n} \frac{\beta^n}{\sqrt{n!}} \mathrm{e}^{-\mathrm{i}r\lambda_l} u_{l,1}u_{l,k+1}|n-k, 3k\rangle \tag{24}$$

and the corresponding density operator:

$$\hat{\rho} = \mathrm{Tr}_p\big(\big|\psi(t)\big\rangle\big\langle\psi(t)\big|\big) = \sum_{j=0}^{\infty}\big\langle j\big|\psi(t)\big\rangle\big\langle\psi(t)\big|j\big\rangle \tag{25}$$

where the trace is made over the Fock states $|j\rangle$ of the pump mode. The Wigner function represented in Fig. 4 is obtained for a pump field in the coherent state $|\beta = 2\rangle$. Such weak pump field is considered in order to reduce the long calculation times. The Wigner function in Fig. 5 shows a star-state shape with interferences that can take negative

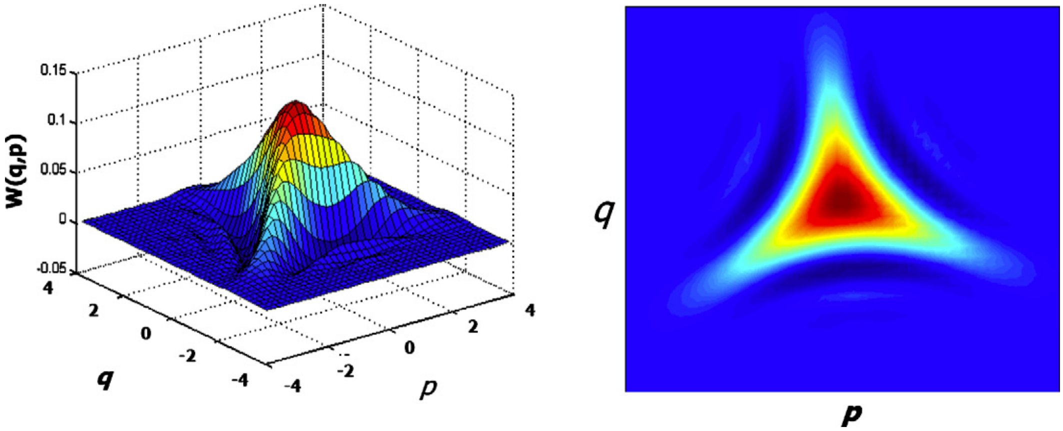

Fig. 4. Wigner function of a degenerate three-photon quantum state for $|\psi(t=0)\rangle = |\beta = 2, 0\rangle$.

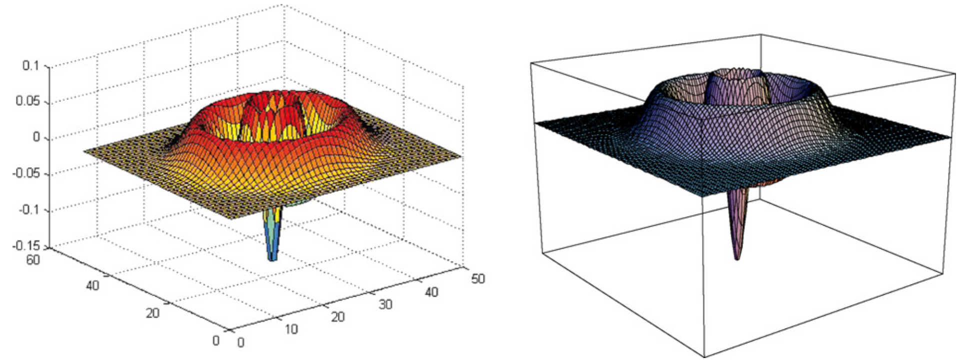

Fig. 5. Left: Wigner function of degenerate triplet photons for a pump field in the Fock number state $|1\rangle$. Right: Wigner function of a Fock number state $|3\rangle$.

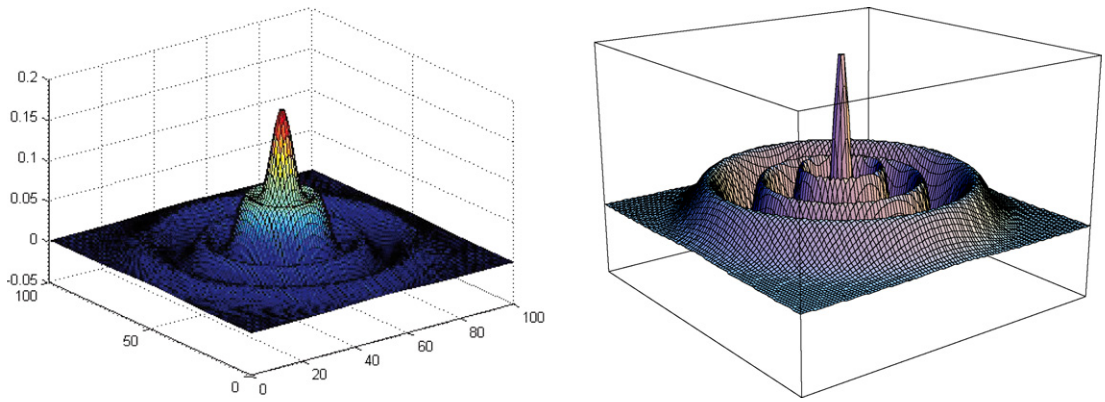

Fig. 6. Left: Wigner function of degenerate triplet photons for a pump field in the Fock number state $|2\rangle$. Right: Wigner function of a Fock number state $|6\rangle$.

values as predicted in Refs. [21,22]. This confirms the validity of our calculations. Moreover, if we consider a pump field in a single photon Fock state $|n_{3\omega} = 1\rangle$, the Wigner function (Fig. 5) associated with the quantum state of the generated three photons is similar to the Wigner function of the Fock state $|n_\omega = 3\rangle$ as we expect. Similarly, we obtain a Wigner function (Fig. 6) close to the one of the Fock state $|n_\omega = 6\rangle$ when the pump field is in the photon number state $|n_{3\omega} = 2\rangle$.

Consider now the situation in which the annihilation of a pump photon leads to the generation of two degenerated photons in the extraordinary mode e and to the creation of a third photon in the ordinary o mode. This situation corresponds to the experimental configuration described in the next paragraph. The quantum state of these photons is given by the wave function (23). The Wigner representation in Fig. 7 of the quantum state of the photons in the e mode is obtained after calculating the density operator traced over the Fock states $|j_p\rangle$ and $|f_o\rangle$ of the pump and ordinary modes:

$$\hat{\rho}_e = \mathrm{Tr}_{p+o}\big(\big|\psi(t)\big\rangle\big\langle\psi(t)\big|\big) = \sum_{j_p=0}^{\infty}\sum_{f_o=0}^{\infty}\big\langle j_p, f_o\big|\psi(t)\big\rangle\big\langle\psi(t)\big|j_p, f_o\big\rangle \tag{26}$$

whereas the Wigner function (Fig. 7) of the quantum state of the photons in mode o is obtained using the density operator:

$$\hat{\rho}_o = \mathrm{Tr}_{p+e}\big(\big|\psi(t)\big\rangle\big\langle\psi(t)\big|\big) = \sum_{j_p=0}^{\infty}\sum_{f_e=0}^{\infty}\big\langle j_p, f_e\big|\psi(t)\big\rangle\big\langle\psi(t)\big|j_p, f_e\big\rangle \tag{27}$$

where the trace operation is made this time over the Fock states $|j_p\rangle$ and $|f_e\rangle$ of the pump and extraordinary modes. Though the Wigner functions of both modes show non-Gaussian shapes, they do not take negative values like the Wigner function of fully degenerated three-photon state.

The ordinary and extraordinary modes are experimentally distinguishable since they have different wavelengths and can thus be separated. The quantum correlations between the quadratures of the two modes can be theoretically estimated using their joint probability distribution defined as:

$$P(X_o, X_e) = \int_{-\infty}^{+\infty}\big|\big\langle\widehat{X}_p, \widehat{X}_o, \widehat{X}_e\big|\psi(t)\big\rangle\big|^2\,\mathrm{d}X_p \tag{28}$$

and represented in Fig. 8 for different pump fields and r parameters. The figure shows cross shaped probability distributions revealing quantum correlations between the o and e mode quadratures. Indeed, when measuring the quadrature of the mode o photons, it is most likely to obtain the same quadrature value for the e mode photons. However, at this stage, the observation of such quantum correlations is strongly limited due to the low efficiency in generating triple photons. This is equivalent to have $r \ll 1$ in our calculations.

5. First experiments in triple photon generation

We considered a triple generation pumped at ω_0 and stimulated by two injection photons, at ω_2 and ω_3. We identified KTP as a good potential material: its third order non-linearity is high, of about $10^{-21}\ \mathrm{m^2/V^2}$ [24], phase-matching is allowed for standard pump wavelengths, and big size crystals with very high optical quality are available. However, our motivation being to generate a pure optical triple state, we have to take care of any possible second order processes which may occur during the wanted third order interaction since KTP is a noncentrosymmetric crystal. Actually, three possible second order cascading interactions with nonzero effective coefficients can occur in the direction of propagation where the third order process is phase-matched:

$$\chi^{(2)}(\omega_2+\omega_3\to\Omega_a):\chi^{(2)}(\omega_0-\Omega_a\to\omega_1),\quad \chi^{(2)}(\omega_0-\omega_2\to\Omega_b):\chi^{(2)}(\Omega_b-\omega_3\to\omega_1)\quad\text{and}$$
$$\chi^{(2)}(\omega_0-\omega_3\to\Omega_c):\chi^{(2)}(\Omega_c-\omega_2\to\omega_1)$$

These interactions can pollute the triple photon experiment because they involve the same incident photons, at ω_0, ω_2, ω_3, and produce photons at ω_1, the generation at the new circular frequencies Ω_a, Ω_b and Ω_c revealing the occurrence of such events. Even if the quadratic processes are not phase-matched, they might be more efficient than the phase-matched cubic process itself because of the relative amplitudes of the $\chi^{(2)}$ and $\chi^{(3)}$ coefficients. It is then of prime importance to minimize the contributions of all the cascading processes. We performed a complete calculation that takes into account both the second- and third-order processes by assuming that the pump and injection beams are undepleted, i.e. $\frac{\partial E(\omega_0)}{\partial Z} = \frac{\partial E(\omega_2)}{\partial Z} = \frac{\partial E(\omega_3)}{\partial Z} = 0$ [25]. It is then possible to calculate the cascading rate, which is the

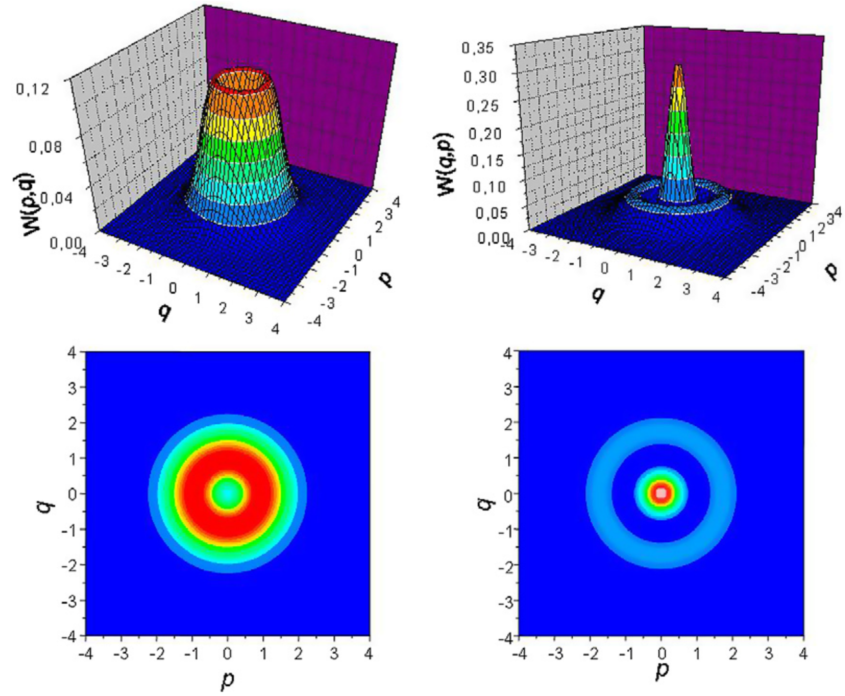

Fig. 7. Left: Wigner function of the photons in the ordinary mode. Right: Wigner function of the photon in the extraordinary mode. For both modes, the pump field is in the coherent state $|\beta = 1\rangle$ and the nonlinear interaction parameter $r = 5.6$.

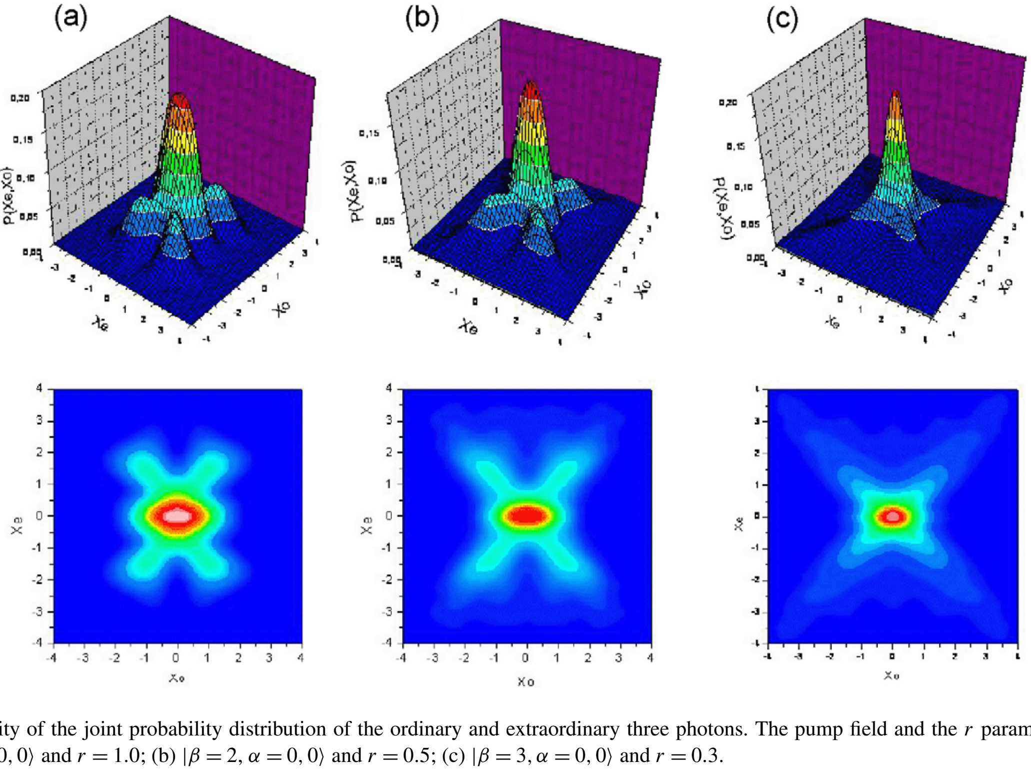

Fig. 8. Density of the joint probability distribution of the ordinary and extraordinary three photons. The pump field and the r parameter are: (a) $|\beta = 1, \alpha = 0, 0\rangle$ and $r = 1.0$; (b) $|\beta = 2, \alpha = 0, 0\rangle$ and $r = 0.5$; (c) $|\beta = 3, \alpha = 0, 0\rangle$ and $r = 0.3$.

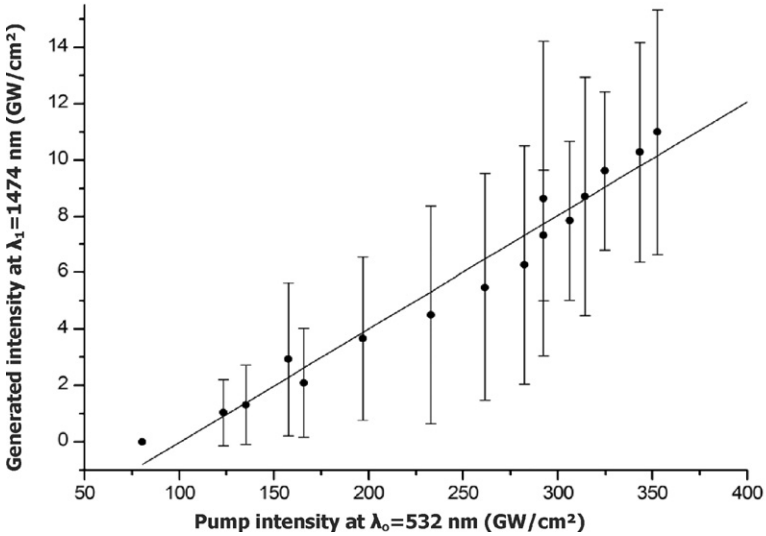

Fig. 9. Generated intensity at $\lambda_1 = 1474$ nm along the X-axis of KTP as a function of the pump intensity at $\lambda_0 = 532$ nm; the injection intensity at $\lambda_2 = \lambda_3 = 1665$ nm is maintained at 100 GW/cm^2. The crystal length is $L = 25$ mm. The circles are the experimental data, and the straight line is the associated linear fit.

ratio between the intensity generated at ω_1 by the cascading process only, $I^{(2)}(\omega_1, Z = L)$, and by the phase-matched third order interaction, $I^{(3)}(\omega_1, Z = L)$ [25]:

$$\eta = \frac{I^{(2)}(\omega_1, Z = L)}{I^{(3)}(\omega_1, Z = L)} = \left(\frac{\sum_i \left(-\frac{\pi}{n(\Omega_i)\cdot\lambda_{\Omega,i}\cdot\cos^2(\gamma(\Omega_i))} \cdot \frac{\chi_{\mathrm{eff},i}^{(2)\text{-I}} \cdot \chi_{\mathrm{eff},i}^{(2)\text{-II}}}{\Delta k_i^{\mathrm{quad}}} \right)}{\chi_{\mathrm{eff}}^{(3)}} \right)^2 \tag{29}$$

where the index $i = a, b, c$ refers to the ith cascading process involving the intermediate circular frequency Ω_i; the phase-mismatch $\Delta k_i^{\mathrm{quad}}$, and the effective coefficients of the two associated quadratic interactions, $\chi_{\mathrm{eff},i}^{(2)\text{-I}}$ and $\chi_{\mathrm{eff},i}^{(2)\text{-II}}$. Note that $\Delta k_i^{\text{quad-I}} = -\Delta k_i^{\text{quad-}II} (= \Delta k_i^{\mathrm{quad}})$ since the $\chi^{(3)}$ process is phase-matched.

Among the seven possible $\chi^{(3)}$ phase-matching types and all the corresponding directions in KTP, we chose to realize the experiment of triple photon generation with the mode combinations $\{-, +, +, -\}$ for $\{n(\omega_0), n(\omega_1), n(\omega_2), n(\omega_3)\}$ and the X-axis because the corresponding third order effective coefficient is maximal, the walk-off angle is nil, the cascading rate is weak, i.e. $\eta = 0.5\%$, and the waves at $\omega_2 = \omega_3$ can be easily separated because their polarizations are orthogonal [25]. The 25-mm-long KTP crystal cut along the X-axis is pumped with a doubled Nd:YAG laser at $\lambda_0 = 532$ nm with a pulse duration of 22 ps (FWHM) and a 10 Hz repetition rate. The injection beam at $\lambda_2 = \lambda_3$ is emitted by a tuneable Optical Parametric Generator pumped with the third harmonic of the Nd:YAG laser. The polarizations of the pump and injection beams are adjusted according to the chosen phase-matching configuration, i.e. $\{-, +, +, -\}$. The injection wavelength $\lambda_2 = \lambda_3$ corresponding to a perfect phase-matching is found at 1665 nm. The wavelength of the associated generated beam is measured at $\lambda_1 = 1474$ nm, which is exactly equal to $(\lambda_0^{-1} - \lambda_2^{-1} - \lambda_3^{-1})^{-1}$ according to the energy conservation. Our photodiode cannot detect any signal at $\lambda_a = 832.5$ nm or at $\lambda_b = \lambda_c = 781.8$ nm that correspond to the intermediate wavelengths involved in the second order cascading processes, while photons at $\lambda_1 = 1474$ nm can be detected. These processes are then negligible with regard to the third order parametric interaction, as expected from the calculation. The measured intensity $I(\lambda_1, Z = L)$ is plotted in Fig. 9 as a function of the pump intensity, $I(\lambda_0, Z = L)$, the injection intensity, $I(\lambda_2, Z = L) + I(\lambda_3, Z = L)$ with $I(\lambda_2, Z = L) = I(\lambda_3, Z = L)$, being maintained at a fixed value of 50 GW/cm^2 [26]. The amount of the generated intensity is such that an undepleted pump and injection approximation can be assumed for the fit. Thus $I(\lambda_1, Z = L)$, which is given by the combination of Jacobian elliptic functions (10), reduces to a simple linear function of the product of the three incident intensities, i.e. $I(\lambda_0, Z = L).I(\lambda_2, Z = L).I(\lambda_3, Z = L)$. These first results are encouraging: we obtained as much as 4.5 μJ/pulse at $\lambda_1 = 1474$ nm, which corresponds to $N(\omega_1, Z = L) = 3.34 \times 10^{13}$ photons/pulse [26]. That means that $3.34 \times 10^{13}\{\omega_1, \omega_2, \omega_3\}$ triple photons/pulse are created, since the generation at

ω_1 is symptomatic of the triple photon generation. Note that the photons at ω_2 and ω_3 that belong to the triple state are mixed with the injection photons, i.e. $N(\omega_2, Z = 0) = 4.19 \times 10^{14}$ photons/pulse and $N(\omega_3, Z = 0) = 4.19 \times 10^{14}$ photons/pulse, the number of pump photons being $N(\omega_0, Z = 0) = 2.0 \times 10^{15}$ photons/pulse.

6. Conclusion

The experiment described in the last section has demonstrated the feasibility of the generation of triple photons in the travelling wave regime based on a double injection scheme in a phase-matched KTP crystal, opening the door to quantum correlations measurements.

Despite of this good result, KTP is probably not the best material for the purpose, the magnitude of its third order electric susceptibility being not so high. The identification of a better phase-matched crystal with a higher cubic nonlinearity is then an open issue. Recently, we shown that TiO_2 rutile could be an interesting candidate, with a figure of merit 7.5 times that of KTP [27]. Furthermore it is a centrosymmetric crystal, so that no quadratic processes able to pollute the triple photons can occur. Other materials, like photonic crystals or fibers have also to be seriously considered.

Finally, by achieving the triple photon generation inside a resonant cavity, which corresponds to a third order optical parametric oscillator, it may be possible to increase the ratio between the generated photons and the injection ones.

References

[1] P. Franken, A.E. Hill, C.W. Peters, G. Weinreich, Generation of optical harmonics, Phys. Rev. Lett. 7 (1961) 118.
[2] R.J. Glauber, Coherent and incoherent states of the radiation field, Phys. Rev. 131 (1963) 2766.
[3] H.P. Yuen, Two-photon coherent states of the radiation field, Phys. Rev. A 13 (1976) 2226.
[4] D.F. Walls, Squeezed states of light, Nature 306 (1983) 141.
[5] A.I. Lvovsky, H. Hansen, T. Aichele, O. Benson, J. Mlynek, S. Schiller, Quantum state reconstruction of the single-photon Fock state, Phys. Rev. Lett. 87 (2001) 050402.
[6] Z.Y. Ou, S.F. Pereira, H.J. Kimble, K.C. Peng, Realization of the Einstein–Podolsky–Rosen paradox for continuous variables, Phys. Rev. Lett. 68 (1992) 3663.
[7] K. Bencheikh, C. Simonneau, J.A. Levenson, Cascaded amplifying quantum optical taps: A robust noiseless optical bus, Phys. Rev. Lett. 78 (1997) 34.
[8] W. Tittel, J. Brendel, H. Zbinden, N. Gisin, Quantum cryptography using entangled photons in energy-time Bell states, Phys. Rev. Lett. 84 (2000) 4737.
[9] D. Bouwmeester, J.-W. Pan, K. Mattle, M. Eibl, H. Weinfurter, A. Zeilinger, Experimental quantum teleportation, Nature 390 (1997) 575.
[10] J.A. Giordmaine, R.C. Miller, Tunable coherent parametric oscillation in $LiNbO_3$ at optical frequencies, Phys. Rev. Lett. 14 (1965) 973.
[11] G.D. Boyd, A. Ashkin, Theory of parametric oscillator threshold with single-mode optical masers and observation of amplification in $LiNbO_3$, Phys. Rev. 146 (1966) 187.
[12] P.N. Butcher, D. Cotter, The Elements of Nonlinear Optics, Cambridge Series in Modern Optics, Cambridge Univ. Press, London, 1990.
[13] B. Boulanger, J.P. Fève, G. Marnier, Field-factor formalism for the study of the tensorial symmetry of four-wave nonlinear optical parametric interactions in uniaxial and biaxial crystal, Phys. Rev. E 48 (1993) 4730.
[14] R. Adair, L.L. Chase, S.A. Payne, Nonlinear refractive index of optical crystals, Phys. Rev. B 39 (5) (1989) 3337–3350.
[15] J.P. Fève, B. Boulanger, J. Douady, Specific properties of cubic optical parametric interactions compared to quadratic interactions, Phys. Rev. A 66 063817 (2002) 1–11.
[16] J.A. Armstrong, N. Bloembergen, J. Ducuing, P.S. Pershan, Interactions between light-waves in a nonlinear dielectric, Phys. Rev. 117 (6) (1962) 1918–1939.
[17] K. Koch, E.C. Cheung, G.T. Moore, S.H. Chakmakjian, J.M. Liu, Hot spots in parametric fluorescence with a pump beam of finite cross section, IEEE J. Quant. Electron. 31 (1995) 769.
[18] U. Leonhardt, Measuring the Quantum State of Light, Cambridge Univ. Press.
[19] G. Breitenbach, T. Müller, S.F. Pereira, J.Ph. Poizat, S. Schiller, J. Mlynek, Squeezed vacuum from a monolithic optical parametric oscillator, J. Opt. Soc. Am. B 12 (1995) 2304;
G. Breitenbach, S. Schiller, J. Mlynek, Measurement of the quantum states of squeezed light, Nature 387 (1997) 471.
[20] D.T. Smithey, M. Beck, M.G. Raymer, Measurement of the Wigner distribution and the density matrix of a light mode using optical homodyne tomography: application to squeezed states and the vacuum, Phys. Rev. Lett. 70 (1993) 1244.
[21] K. Banaszek, P.L. Knight, Quantum interference in three-photon down-conversion, Phys. Rev. A 55 (1997) 2368.
[22] T. Felbinger, S. Schiller, J. Mlynek, Oscillation and generation of nonclassical states in three-photon down-conversion, Phys. Rev. Lett. 80 (1998) 492.
[23] D.F. Walls, R. Barakat, Quantum-mechanical amplification and frequency conversion with a trilinear Hamiltonian, Phys. Rev. A 1 (1970) 446.
[24] B. Boulanger, J.P. Fève, P. Delarue, I. Rousseau, G. Marnier, Cubic optical nonlinearity of $KTiOPO_4$, J. Phys. B: At. Mol. Opt. Phys. 32 (1999) 475–488.

[25] J. Douady, B. Boulanger, Calculation of quadratic cascading contributions associated with a phase-matched cubic frequency difference generation in a $KTiOPO_4$ crystal, J. Opt. A: Pure Appl. Opt. 7 (2005) 467–471.
[26] J. Douady, B. Boulanger, Experimental demonstration of a pure third-order optical parametric downconversion process, Opt. Lett. 29 (23) (2004) 2794–2796.
[27] F. Gravier, B. Boulanger, Phase-matched third-order frequency generation in TiO_2 rutile single crystal, in: Conference on Laser and Electro-Optics, Long Beach California, 21–26 May 2006.